Research Article

Hydrogen gas therapy: A promising approach for sepsis management post-burn injury by modulating inflammation, oxidative stress, and wound healing

Pan Yu, MD[1]*, Nan Hong, MD[1], Genwang Wang, BS[2], Shuqiang Chen, MS[1], Zhipeng Zhao, MS[1]

Departments of [1]Burn and Plastic Surgery, [2]Scientific Research and Training, Jinling Hospital, Affiliated Hospital of Medical School, Nanjing University, Nanjing, China.

*Corresponding author:

Pan Yu,
Department of Burn and Plastic Surgery, Jinling Hospital, Affiliated Hospital of Medical School, Nanjing University, Nanjing, China.

yp52@163.com

ABSTRACT

Objective: Burns refers to a severe form of trauma that often leads to localized and systemic inflammatory responses, oxidative stress, and immune dysfunction. Patients with severe burns are highly susceptible to the development of postburn sepsis, a condition influenced by multiple factors, such as bacterial infection of the burn wound, alterations in immune status, and excessive release of inflammatory mediators. This study aimed to investigate the mechanisms by which hydrogen gas treatment exerts its effects on postburn sepsis, with a focus on its influence on inflammatory responses, oxidative stress, and wound healing.

Material and Methods: This work employed *in vitro* assays with Sprague–Dawley (SD) rat skin fibroblasts (RSFs) to assess the effects of burn serum and hydrogen gas on cell proliferation through methylthiazolyldiphenyl-tetrazolium bromide assays and on apoptosis through flow cytometry with Annexin V-fluorescein isothiocyanate/propidium iodide staining. In addition, an enzyme-linked immunosorbent assay was performed to quantify inflammatory cytokines and oxidative stress markers in fibroblasts treated with burn serum. Western blotting (WB) analysis was conducted to investigate signaling pathway modulation. The severe burn sepsis models of SD rats were segregated into three experimental groups: a healthy normal control group, a burn sepsis control group, and a burn sepsis + hydrogen gas (2%) treatment group. Wound healing was monitored, with wound contraction rates recorded and histological assessments conducted using hematoxylin and eosin and Masson's trichrome staining to evaluate tissue repair and collagen deposition.

Results: *In vitro* assays showed that burn serum reduced fibroblast proliferation and increased apoptosis ($P < 0.01$), which hydrogen gas mitigated by rescuing cell viability and reducing apoptosis ($P < 0.01$). Enzyme-linked immunosorbent assay revealed burn serum-induced increases in the levels of inflammatory cytokines and oxidative stress markers, with decreases in antioxidant enzymes ($P < 0.01$), which hydrogen gas reversed ($P < 0.05$). WB analysis suggested hydrogen gas's anti-inflammatory and proliferative effects by modulating signaling pathways ($P < 0.01$). *In vivo*, hydrogen gas treatment considerably improved wound healing, with accelerated contraction and enhanced collagen deposition. Plasma and skin tissue analyses indicated systemic and local anti-inflammatory and antioxidant effects from hydrogen gas.

Conclusion: Hydrogen gas treatment demonstrates potential therapeutic efficacy in the management of postburn sepsis by modulating inflammatory responses, reducing oxidative stress, and promoting wound healing. These findings provide scientific evidence supporting hydrogen gas as an adjunctive treatment strategy for postburn sepsis.

Keywords: Burn sepsis, Hydrogen therapy, Inflammatory response, Oxidative stress, Wound healing

INTRODUCTION

Burns represents a severe form of trauma that often triggers complex pathophysiological changes, including local and systemic inflammatory responses, oxidative stress, and immune dysfunction.[1,2] Patients with severe burns are highly susceptible to the development of postburn sepsis, a condition influenced by multiple factors, such as bacterial infection of the burn wound, alterations in immune status, and excessive release of inflammatory mediators.[3,4] These factors cumulatively promote the onset of systemic inflammatory response syndrome and multiple organ dysfunction syndrome, which may further advance to septic shock and ultimately result in fatality.[5] The pathogenesis of burn sepsis is complex and involves the abnormal activation and regulation of multiple signaling pathways. The nuclear factor-kappa B (NF-κB), mitogen-activated protein kinase (MAPK), Janus kinase-signal transducer and activator of transcription, phosphatidylinositol 3-kinase/protein kinase B, glycogen synthase kinase-3, and cholinergic anti-inflammatory pathways are all implicated in the development of sepsis.[6-10] Despite the progress in the treatment of sepsis in modern medicine, the mortality rate of this condition following burns remains high.[11] Therefore, the identification of effective therapeutic strategies to improve the prognosis of postburn sepsis is a critical focus of current clinical research.

Hydrogen gas (H₂) has gained considerable attention as a novel medicinal gas due to its unique biological properties. Hydrogen possesses strong antioxidant capabilities and can selectively neutralize harmful free radicals, such as hydroxyl radicals and peroxynitrite, which reduce oxidative damage.[12] Moreover, hydrogen's anti-inflammatory properties have been widely recognized because they can modulate various inflammation-related signaling pathways and alleviate inflammatory responses.[13] In the context of burns, the complexity of wound healing – which involves the infiltration of inflammatory cells, cell proliferation, collagen deposition, and tissue remodeling – cannot be overlooked.[14,15] The beneficial effects of hydrogen on wound healing likely stem from its anti-inflammatory and antioxidant properties, although the precise mechanisms remain to be fully elucidated.[16,17] Hydrogen promotes wound healing by regulating cell signaling, enhancing cell proliferation and differentiation, and inhibiting apoptosis.[18] It has been reported that hydrogen exerts anti-inflammatory effects through the Nrf2/HO-1 signaling pathway, reducing the mortality rate of septic rats.[19,20] In addition, hydrogen therapy decreased the levels of high mobility group box 1 (HMGB1) protein in model animals, which further confirmed its anti-inflammatory effects.[21] Moreover, hydrogen has shown certain therapeutic effects on the adjunctive treatment of clinical diseases, such as diabetes, metabolic syndrome, gout, cardiovascular and cerebrovascular diseases, and tumors, which demonstrate its potential medical application value as a new type of biomedical molecular gas.[22]

In this research, our objective was to explore the therapeutic benefits of hydrogen in the treatment of a rat model of severe burn sepsis and its influence on wound recovery. Through a series of experiments, including cell culture, molecular biology assays, and histological evaluations, we assessed hydrogen's regulatory effects on inflammation, oxidative stress, and wound healing. This study will deepen our understanding and provide evidence supporting the use of hydrogen in postburn sepsis treatment, presenting a promising new therapeutic approach for burn patients.

MATERIAL AND METHODS

Sprague–Dawley (SD) rat burn model induction

Twenty-seven male Sprague-Dawley rats aged 6-8 weeks with body weights of 180-200 g, along with three male neonatal SD rats aged 3 weeks weighing approximately 50 g, were procured from Changzhou Kavin Biological. The rats were housed in individually ventilated plastic cages in a humidified environment (room temperature: 20-26°C relative humidity: 50-60%, air flow: 150 CFM) in a pathogenic-free laboratory. Before the initiation of the experiments, the study was approved by an authorized institutional review board, the Institutional Animal Care and Use Committee of Jinling Hospital, Affiliated Hospital of Medical School, Nanjing University, China. (Approval Number: DBZQZYY23BBJ0081). Although the research subjects are rats and cannot provide explicit consent, all experimental procedures were designed to adhere to the principles of laboratory animal welfare and were carried out under the premise of minimizing potential harm and discomfort to the animals. Every effort was made to ensure that the use of these animals in the study met high - level ethical standards, in line with the requirements of both national and international ethical norms for animal research.

The rats were anesthetized via intraperitoneal injection of sodium pentobarbital (40 mg/kg, 20 mg/mL, P3761, Merck, Darmstadt, Germany).[23] Following depilation with sodium sulfide, a circular area (5 cm in diameter) of shaved dorsal skin was immersed in 92°C water for 18 seconds to induce full-thickness third-degree burns.[24] Post-injury resuscitation was performed through intraperitoneal administration of compound sodium chloride (40 mL/kg, R20263, Yuanye Biotechnology, Shanghai, China). One hour after resuscitation, lipopolysaccharide solution (10 mg/kg, 10 mg/mL, ST1470, Beyotime Biotechnology, Shanghai, China) was administered intraperitoneally.

Rat serum preparation

Twelve rats were evenly divided into two groups, with one group undergoing induction of a burn rat model to collect burn rat serum and the other group being normally raised to collect normal rat serum. At 24 h postburn, the rats were euthanized by administering sodium pentobarbital (150 mg/kg, 20 mg/mL, P3761, Merck, Darmstadt, Germany) through intraperitoneal injection. Their blood was collected into sterile tubes. The blood samples were allowed to clot at room temperature for 2 h, followed by centrifugation (5406000092, Eppendorf, Hamburg, Germany) at 1000g for 15 min to isolate the serum. Serum was carefully aspirated to avoid clot contamination. Samples from rats in the same experimental group were pooled, aliquoted into cryovials, and stored at −80°C for subsequent analysis.[25,26]

RSF extraction

Three 3-week-old male neonatal SD rats, weighing around 50 g, were procured from Changzhou Kavin Biological. Before the initiation of the experiments, neonatal rats were euthanized by administering sodium pentobarbital (150 mg/kg, 20 mg/mL, P3761, Merck, Darmstadt, Germany) through intraperitoneal injection. The skin was disinfected in 75% ethanol for 3–5 min to prevent microbial contamination. Then, it was carefully excised and minced into 1×1 mm³ pieces. A mixed enzyme solution was used to digest the minced tissue at 37°C for 30–45 min to facilitate the release of fibroblasts. The digested tissue was gently pipetted to dislodge the cells, which were then centrifuged at 1500 rpm for 5 min. The resulting cell pellet was resuspended in Dulbecco's Modified Eagle Medium/F12 complete medium (SH30023.02, Hyclone, Logan, Utah, USA) and cultured in a humidified incubator (8000, Thermo Scientific, Waltham, MA, USA) at 37°C with 5% carbon dioxide. All cell cultures were free from mycoplasma infection. Immunofluorescence staining was performed to identify the cells with Alexa Fluor® 594-Vimentin antibody (1:1000 dilution, ab154207, Abcam, Cambridge, England). A fluorescence inverted microscope (DMI3000B, Leica, Germany) was used to obtain visual images.[27]

Immunofluorescence staining assay

Rat cells were cultivated to 60–70% and then fixed with 4% paraformaldehyde at room temperature for 20 min. Subsequently, the cells were permeabilized with 0.1% Triton X-100 (T8200, Solarbio, Beijing, China) at room temperature for 5 min to facilitate the penetration of antibodies. Afterward, the cells were blocked with 3% bovine serum albumin (ST023, Beyotime Biotechnology, Shanghai, China) at room temperature for 30 min to reduce non-specific binding. Then, the cells were incubated with the Alexa Fluor® 594-Vimentin antibody (1:1000 dilution, ab154207, Abcam,

Cambridge, England) overnight at 4°C. On the following day, the cell nuclei were stained with Hoechst 33342 (diluted 1:100, C1029, Beyotime Biotechnology, Shanghai, China) at room temperature for 5 min. Subsequently, the cells were observed and photographed using a fluorescence-inverted microscope (DMI3000B, Leica, Germany).[28]

Methylthiazolyldiphenyl-tetrazolium (MTT) bromide assay

RSF cells were seeded at 4×10^4 cells/mL in a 96-well plate and incubated for 24 h for attachment and growth. Then, the RSF cells were treated with fetal bovine serum (FBS) (SH30406.03, Hyclone, Logan, Utah, USA), FBS, and hydrogen gas (generated using a hydrogen generator, AYAN-HC500ML, AnYan Instrument, Hangzhou, China), burned rat serum, burned rat serum and hydrogen gas, normal rat serum, and normal rat serum and hydrogen gas separately. After treatment of 48 h, 15 μL MTT (M5655, St. Louis, MO, USA) was added per well and incubated an additional 4 h at 37°C. The supernatant was aspirated, and 200 μL dimethyl sulfoxide (D12345, Invitrogen, Thermo Fisher Scientific, Massachusetts, USA) was added to dissolve formazan crystals. Absorbance was measured at 492 nm using a microplate reader (TDZ4B-WS, Lu Xiangyi Centrifuge Instrument, Shanghai, China).

Flow cytometry for apoptosis detection

RSF cells were seeded in a 6-well plate at a density of 1×10^5 cells/mL and cultured for 24 h to reach a semiconfluent state. Then, RSF cells were treated with FBS (SH30406.03, Hyclone, Logan, Utah, USA), FBS and hydrogen gas (generated using a hydrogen generator, AYAN-HC500ML, AnYan Instrument, Hangzhou, China), burned rat serum, burned rat serum and hydrogen gas, normal rat serum, and normal rat serum and hydrogen gas separately. After treatment for 48 h, the cells were collected, washed with cold phosphate-buffered saline (PBS), and stained with Annexin V-fluorescein isothiocyanate/propidium iodide (Annexin V-FITC/PI) Apoptosis Detection Kit (401006, BeiBo Biological Technology, Nanjing, China), in accordance with the manufacturer's protocol, to detect apoptotic cells. The stained cells were then analyzed using a flow cytometer (FACSVerse, Becton, Dickinson and Company, Franklin Lakes, NJ, USA), and the data were processed using FlowJo (v10.6.2, Becton, Dickinson and Company, Franklin Lakes, NJ, USA).[29,30]

Enzyme-linked immunosorbent assay (ELISA) for cytokine and oxidative stress markers

RSF cells were plated at 3×10^4 cells/mL in a 48-well plate, cultured for 24 h, and then treated with FBS (SH30406.03, Hyclone, Logan, Utah, USA), FBS and hydrogen gas (generated using a hydrogen generator, AYAN-HC500ML, AnYan

Instrument, Hangzhou, China), burned rat serum, burned rat serum and hydrogen gas, normal rat serum, and normal rat serum and hydrogen gas separately for another 48 h. Supernatants were collected and stored at −80°C pending ELISA analysis. For skin tissue samples obtained from animal experiments, the tissue was first cut into small pieces using scissors and then added with PBS (PB180327, Pricella, Wuhan, China). The tissue was then homogenized using a homogenizer (357544, Wheaton, Millville, USA). After homogenization, the samples were subjected to low-speed centrifugation (1000 g, 15 min, 5406000092, Eppendorf, Hamburg, Germany) to collect the supernatant and stored at −80°C for subsequent analysis. The levels of HMGB1, interleukin (IL)-6, malondialdehyde (MDA), IL-1β, tumor necrosis factor-alpha (TNF-α), superoxide dismutase (SOD), and glutathione (GSH) were quantified using the corresponding ELISA kits (JL13892, JONLNBIO, Shanghai, China; A003-1, Jiancheng Bioengineering Research Institute, Nanjing, China; A001-3, Jiancheng Bioengineering Research Institute, Nanjing, China; A006-1, Jiancheng Bioengineering Research Institute, Nanjing, China; E-EL-R0015, Elabsciece, Wuhan, China; E-EL-R0012, Elabsciece, Wuhan, China; E-EL-R2856, Elabsciece, Wuhan, China, respectively), in accordance with the manufacturer's instructions. The absorbance was measured at specified wavelengths using a microplate reader (TDZ4B-WS, Lu Xiangyi Centrifuge Instrument, Shanghai, China), and the concentrations of the markers were determined through comparison of the absorbance values to the standard curves provided with the kits.

Western blotting (WB) analysis

RSF cells were seeded in a 6-well plate at a density of 1 × 10^5 cells/mL and cultured for 24 h. Then, RSF cells were treated with FBS (SH30406.03, Hyclone, Logan, Utah, USA), FBS and hydrogen gas (generated using a hydrogen generator, AYAN-HC500ML, AnYan Instrument, Hangzhou, China), burned rat serum, burned rat serum and hydrogen gas, normal rat serum, and normal rat serum and hydrogen gas separately for 48 h. Cells were collected and lysed in radioimmunoprecipitation assay buffer (P0013B, Beyotime Biotechnology, Shanghai, China) containing phenylmethylsulfonyl fluoride to inhibit protease activity. Protein concentrations were determined using a BCA protein assay kit (KGDBCA, Keygen, Jiangsu, China), and equal amounts of protein from each sample were loaded onto sodium dodecyl sulfate-polyacrylamide gel electrophoresis gels for electrophoresis. After separation, the proteins were transferred to polyvinylidene fluoride membranes (FFP32, Beyotime Biotechnology, Shanghai, China), which were then blocked with 5% skim milk in Tris-buffered saline with Tween 20 to prevent non-specific binding.[31] The membranes were incubated with phospho-extracellular signal-regulated kinase (p-Erk1/2) antibody (1:1000 dilution, 4370, Cell Signaling Technology, MA,USA), Erk1/2 antibody (1:1000 dilution,

4695, Cell Signaling Technology, MA,USA), phosphorylated c-Jun N-terminal kinase (p-JNK) antibody (1:1000 dilution, 9251, Cell Signaling Technology, MA,USA), c-Jun N-terminal kinase (JNK) antibody (1:1000 dilution, 9252, Cell Signaling Technology, MA,USA), phosphorylated nuclear factor kappa-B (p-NF−κB) antibody (1:1000 dilution, 3033, Cell Signaling Technology, MA,USA), Nuclear Factor kappa-B (NF-κB) antibody ((1:1000 dilution, 8242, Cell Signaling Technology, MA,USA), p-p38 antibody (1:1000 dilution, 9211, Cell Signaling Technology, MA,USA), p-38 antibody (1:1000 dilution, 9212, Cell Signaling Technology, MA,USA), glyceraldehyde-3-phosphate dehydrogenase antibody (1:10000 dilution, 2118S, Cell Signaling Technology, MA, USA), and β-actin antibody (1:10000, 4967, Cell Signaling Technology, MA, USA) overnight at 4°C, followed by incubation with horse radish peroxidase-conjugated secondary antibodies(ab7090, Abcam, Cambridge, England). The membrane was removed from the secondary antibody solution and washed 3 times with TBST (ST671, Beyotime Biotechnology, Shanghai, China) for 5 min each time to remove unbound antibodies. The A and B components of the ECL reagent (P0018AM, Beyotime Biotechnology, Shanghai, China) were mixed in equal volume proportions. The mixture was then evenly applied to the surface of the membrane at a rate of 1 ml per 10 cm^2 and incubated for 1–2 min. Protein bands were visualized using an integrated chemiluminescence imager (ChemiScope 5300 Pro, Qinxiang Scientific Instrument, Shanghai, China), and band intensity was quantified using ImageJ (1.6.0-20, National Institutes of Health, USA).

Hydrogen gas treatment of animal models

The SD rats were randomly divided into three groups, namely, the healthy control, burn sepsis, and burn sepsis plus hydrogen treatment groups, with five rats in each group. The burn sepsis model was constructed following the aforementioned procedures. For hydrogen treatment, the rats were housed in a sealed chamber equipped with a hydrogen gas generator that mixed hydrogen with air at a flow rate of 4 L/min. The rats were exposed to 65% hydrogen gas for 2 h daily, starting 3 h after resuscitation. The concentration and exposure time were selected based on preliminary studies to ensure the effectiveness of hydrogen gas treatment.[32,33] On days 1, 3, 7, 14, and 20 postburn treatment, photographs, and records of the dorsal burn area of the rats were captured and documented, respectively.

Hematoxylin and eosin (HE) staining and Masson's trichrome staining

At 20 days postburn treatment, the dorsal skin tissues of SD rats were carefully excised from the animals, and skin samples from the control, burn sepsis, and burn sepsis plus hydrogen treatment groups were individually labeled for each group. Skin tissues were fixed in 10% formalin to preserve the tissue

structure, dehydrated in a graded series of ethanol, cleared in xylene, and embedded in paraffin. Sections were cut and stained through HE staining (G1120, Solarbio, Beijing, China) for histological examination to visualize cellular morphology and tissue architecture. For Masson's trichrome staining, the sections were stained with Weigert's iron hematoxylin followed by aniline blue and orange G (G1346, Solarbio Beijing, China) to visualize collagen deposition and arrangement and gain insights into the extracellular matrix composition and tissue remodeling.[34]

Statistical analysis

All experiments were performed in triplicate to ensure reproducibility, and the data are presented as the mean ± standard deviation. Statistical analysis was performed using one-way analysis of variance followed by t-tests for multiple comparisons. $P < 0.05$ was considered statistically significant, which indicates a meaningful difference between groups. All line charts and bar graphs were analyzed using GraphPad (9.5.0, GraphPad Software, San Diego, USA).

RESULTS

Hydrogen gas effectively mitigated burn serum-induced reductions in fibroblast proliferation and enhanced apoptosis

Fibroblasts extracted from the skin tissues of SD rats were imaged under a microscope, and they displayed morphological characteristics, including spindle and polygonal shapes, large cell bodies, central oval or elliptical nuclei, and multiple protuberances of varying sizes extending from the cytoplasm. During growth, the cells exhibited a radially flamelike or vortical pattern, which indicates cellular health and activity [Figure 1a]. Fluorescence staining revealed the presence of vimentin, a fibroblast cytoskeletal protein, which confirmed the correct extraction of the RSF cells [Figure 1b].

To investigate the effects of burn serum from rat models and hydrogen gas on fibroblast proliferation and growth inhibition, we randomly allocated twelve SD rats into two groups: the burned rat serum group and the normal rat serum group, with six rats in each group. For the establishment of the burn sepsis model, the rats in the burned rat serum group were exposed to 92°C hot water, and those in the normal rat serum group were treated with 37°C warm water. Serum samples were collected from all rats 24 h posttreatment and stored for subsequent experimental analysis. MTT assays were conducted on fibroblasts under different conditions: normal FBS, normal FBS supplemented with hydrogen gas, burn serum, burn serum supplemented with hydrogen gas, normal rat serum, and normal rat serum supplemented with hydrogen gas. The results reveal that the burn serum significantly reduced cell proliferation ($P < 0.01$). Notably, the addition of hydrogen gas in the burn serum group mitigated this detrimental effect,

which suggests the protective role of hydrogen gas against burn-related cytotoxicity ($P < 0.01$). Hydrogen gas also improved cellular responses in normal rat serum, which further supports this protective effect and highlights the potential therapeutic utility of hydrogen gas in modulating cellular responses and promoting wound healing [Figure 1c and d].

To further explore the effects of burn serum and hydrogen gas on cell apoptosis, we employed flow cytometry using Annexin V-FITC and PI double staining to provide quantitative and visual data on apoptosis. The results show that 10% burn serum-induced apoptosis (15.91%) in cells after 24 h compared with normal cells. Co-treatment with 60% hydrogen gas significantly reduced the apoptosis rate (10.9%) in the burn serum group ($P < 0.01$). Dot plots were used to visualize the distribution of live cells, early apoptotic cells, late apoptotic cells, and necrotic cells. The burn serum-treated group exhibited a clear trend toward apoptosis, which was reversed in the presence of hydrogen gas [Figure 1e and f]. These findings collectively demonstrate that burn serum negatively affected fibroblast proliferation and survival, and hydrogen gas treatment counteracted these effects by promoting cell proliferation and inhibiting apoptosis, which suggests a potential therapeutic role for hydrogen gas in modulating cellular responses in burn wound healing.

Hydrogen gas reduces inflammation and oxidative stress in fibroblasts treated with burn serum

To investigate the effects of burn serum and hydrogen gas treatment on inflammation and oxidative stress in fibroblasts, we employed ELISA to assess changes in the cytokine levels of the cell culture media. Inflammatory markers, including TNF-α [Figure 2a], IL-1β [Figure 2b], IL-6 [Figure 2c], and HMGB1 [Figure 2d], showed significantly elevated levels in fibroblast cultures compared with the normal FBS group ($P < 0.01$). This increase indicates a pronounced inflammatory response. Notably, the addition of hydrogen gas to the culture media resulted in a significant reduction in the levels of these cytokines ($P < 0.05$), which suggests that hydrogen gas may possess anti-inflammatory properties and potentially attenuate the inflammatory response to fibroblasts. Oxidative stress markers, including MDA [Figure 2e], SOD [Figure 2f], and GSH [Figure 2g], were also evaluated. Results suggest increased levels of MDA, which is an indicator of lipid peroxidation, which implies enhanced oxidative stress in the fibroblast cultures. Conversely, SOD activity and GSH levels, which are crucial for antioxidant defense, were reduced in the cultures ($P < 0.01$). The supplementation of hydrogen gas led to decreased MDA levels and increased SOD activity and GSH levels ($P < 0.01$), which indicate the protective effect of hydrogen gas against oxidative stress. These results demonstrate that hydrogen gas can modulate inflammation and oxidative stress responses in fibroblast cultures treated with burn serum.
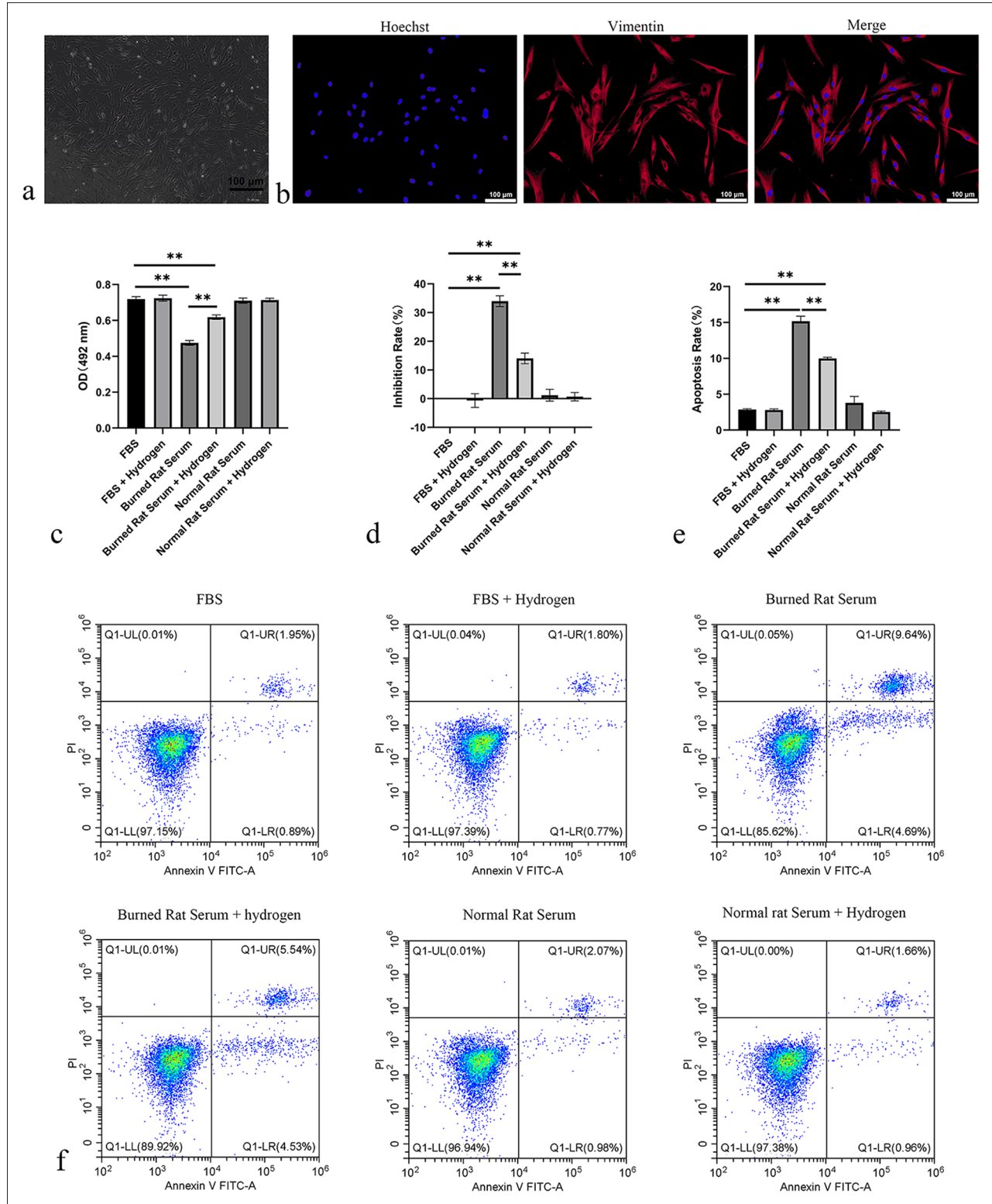
Figure 1: Effects of burn serum and hydrogen gas treatment on fibroblast proliferation and apoptosis. (a) Photographs of the morphology of extracted fibroblasts; (b) immunofluorescence staining results for RSF cells (Hoechst and Vimentin) were obtained at a magnification of 200x; (c) MTT assay examining the effects of burn serum and hydrogen gas on fibroblast proliferation, $n = 3$; (d) MTT assay assessing the influence of burn serum and hydrogen gas on the growth inhibition of fibroblasts, $n = 3$; (e) quantitative analysis of flow-cytometry dual staining for determining the influence of burn serum and hydrogen gas on fibroblast apoptosis, $n = 3$; and (f) dot plots from flow-cytometry dual staining depicting the effects of burn serum and hydrogen gas on fibroblast apoptosis. **$P < 0.01$. FBS: Fetal bovine serum; RSF cells: Rat skin fibroblasts, MTT: Methylthiazolyldiphenyl-tetrazolium.
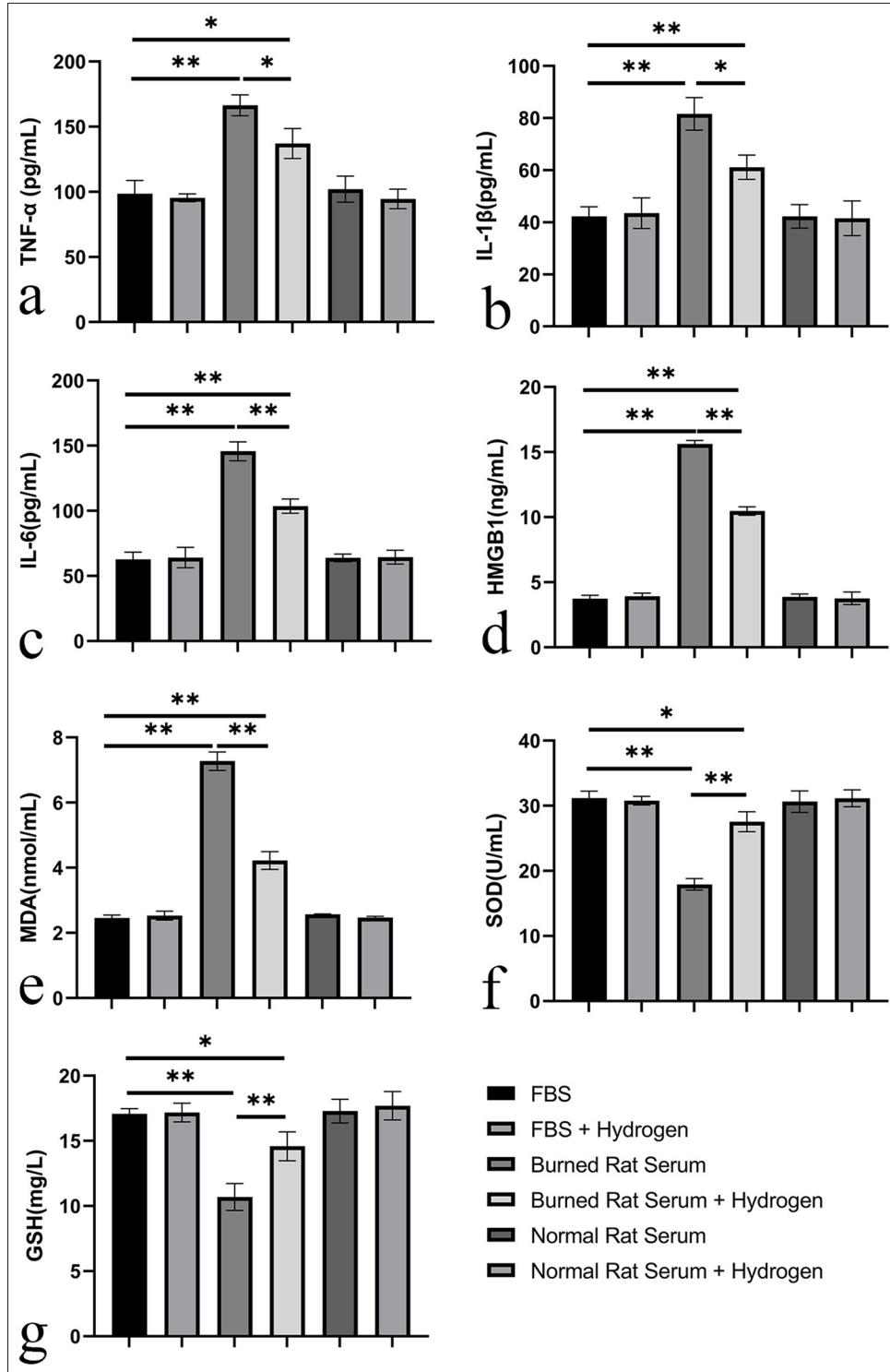
Figure 2: Evaluation of cytokine levels in fibroblast cultures using ELISA. (a) TNF-α, (b) IL-1β, (c) IL-6, (d) HMGB1, (e) MDA, (f) SOD; and (g) GSH. *$P < 0.05$, **$P < 0.01$, compared with the normal FBS group, $n = 3$. ELISA: Enzyme-linked immunosorbent assay, MDA: Malondialdehyde, SOD: Superoxide dismutase, GSH: Glutathione, HMGB1: High-mobility group box 1 protein, FBS: Fetal bovine serum, IL-1β: Interleukin 1 beta, TNF-α: Tumor necrosis factor-alpha.

H₂ treatment modulates key signaling pathways in fibroblasts related to inflammation and stress responses, potentially facilitating inflammatory resolution and promoting cellular homeostasis post-burn

To elucidate the molecular mechanisms by which burn serum and hydrogen gas treatment regulate fibroblast responses, we employed WB and quantitative protein analysis to detect key marker proteins and their phosphorylation changes involved in cellular signaling related to inflammation, stress, and proliferation [Figure 3a]. Compared with the normal FBS group, fibroblasts treated with burn serum exhibited a significantly increased ratio of p-Erk1/2 to Erk1/2 ($P < 0.01$), which indicates the activation of the Erk1/2 pathway. This activation is consistent with the known role of Erk1/2 in cellular responses to stress and injury.[35] Hydrogen gas treatment decreased this ratio ($P < 0.01$), which suggests a potential inhibitory effect on the prosurvival signaling cascade [Figure 3b]. After burn injury, the activation of Erk1/2, a member of the MAPK family, may be associated with the cell's response to damage and the repair process. We hypothesize that the therapeutic effects of hydrogen gas on the regulation of ERK1/2 signaling pathway molecule expression may be involved in the wound healing process.[36] JNK, another member of the MAPK family, contributes to cellular stress, inflammation, and apoptosis.[37] Burn serum treatment resulted in a marked increase in the p-JNK to JNK ratio ($P < 0.01$), which reflects the activation of the JNK stress signaling pathway. The activation of JNK may be related to cellular stress response and the production of inflammatory mediators. Hydrogen gas treatment significantly reduced this ratio ($P < 0.01$), which indicates the protective effect of hydrogen gas against stress-induced cellular damage [Figure 3c]. Exposure to burn serum increased the ratio of p-NF-κB to NF-κB in fibroblasts ($P < 0.01$), which implies the activation of the NF-κB pathway, a central regulator of inflammation. Hydrogen gas treatment effectively decreased this ratio ($P < 0.01$), which suggests an anti-inflammatory effect exerted through the inhibition of the NF-κB signaling pathway [Figure 3d]. The activation of NF-κB may lead to increased expressions of pro-inflammatory cytokines, which trigger and exacerbate inflammatory response. Previous studies have shown the importance of NF-κB in burn healing by demonstrating the promotional effect of inhibiting the NF-κB pathway on rat burn wound healing.[10] Burn serum treatment significantly upregulated the p-P38 to P38 ratio in fibroblasts ($P < 0.01$), which activated the P38 pathway involved in the regulation of inflammation and cellular death. Hydrogen gas treatment markedly reduced this ratio ($P < 0.01$), which indicates a mitigating effect on the inflammatory response [Figure 3e]. Following a burn, the activation of P38 may show an association with the production of inflammatory cytokines and apoptosis. The role and mechanism of p38 in systemic inflammatory response after severe burn and its function

in acute lung injury in burned rats indicate the significant involvement of the P38 signaling pathway in the pathological response and healing process after burn injury.[36,38]

Hydrogen gas treatment-enhanced wound contraction and histological outcomes in burn sepsis rats

To further investigate the therapeutic effects of hydrogen gas on burn sepsis, particularly its role in promoting wound healing, we randomly assigned the SD rats to three distinct groups: the normal control, burn sepsis, and burn sepsis + H₂ groups, with each group comprising five rats. For the establishment of the burn sepsis model, the SD rats in the burn sepsis and burn sepsis + H₂ groups were subjected to a 92°C hot water bath. By contrast, the normal control group received a 37°C warm water bath. Wound size was recorded, and healing curves were plotted to clearly depict the wound healing process, with the X-axis representing days post-injury and the Y-axis showing the percentage of wound contraction. Wound contraction rates were significantly lower in the burn sepsis control group compared with the burn sepsis + H₂ group, which indicates delayed wound healing without hydrogen gas treatment ($P < 0.01$). The burn sepsis + hydrogen gas group exhibited notably accelerated wound contraction rates, with a stable increase in wound closure rates from day 1 to day 20 postinjury. This trend suggests that hydrogen gas treatment significantly accelerated the wound-healing process in burn sepsis [Figure 4a]. Histological assessments of wound healing through HE staining and Masson's trichrome staining are presented in Figures 4b and c, respectively. The HE staining results show that 20 days after the construction of the burn sepsis model, structural changes in the wound varied significantly between the control and treatment groups. The burn sepsis group showed abundant inflammatory cells within newly formed granulation tissue, disorganized collagen fibers, and sparse new blood vessels. By contrast, the group treated with H₂ showed improved re-epithelialization [Figure 4b]. Masson's trichrome staining highlighted collagen deposition and tissue organization within the wound area. The burn sepsis control group presented scattered and loosely arranged collagen fibers, and the H₂-treated group displayed substantial improvements, including an increased amount of collagen and a denser and more orderly collagen matrix. These findings indicate that hydrogen gas treatment not only enhanced wound closure rates but also the quality of tissue repair by promoting the orderly deposition of collagen [Figure 4c].

Hydrogen gas treatment-modulated inflammatory and oxidative stress responses in plasma and skin tissue of burn sepsis rats

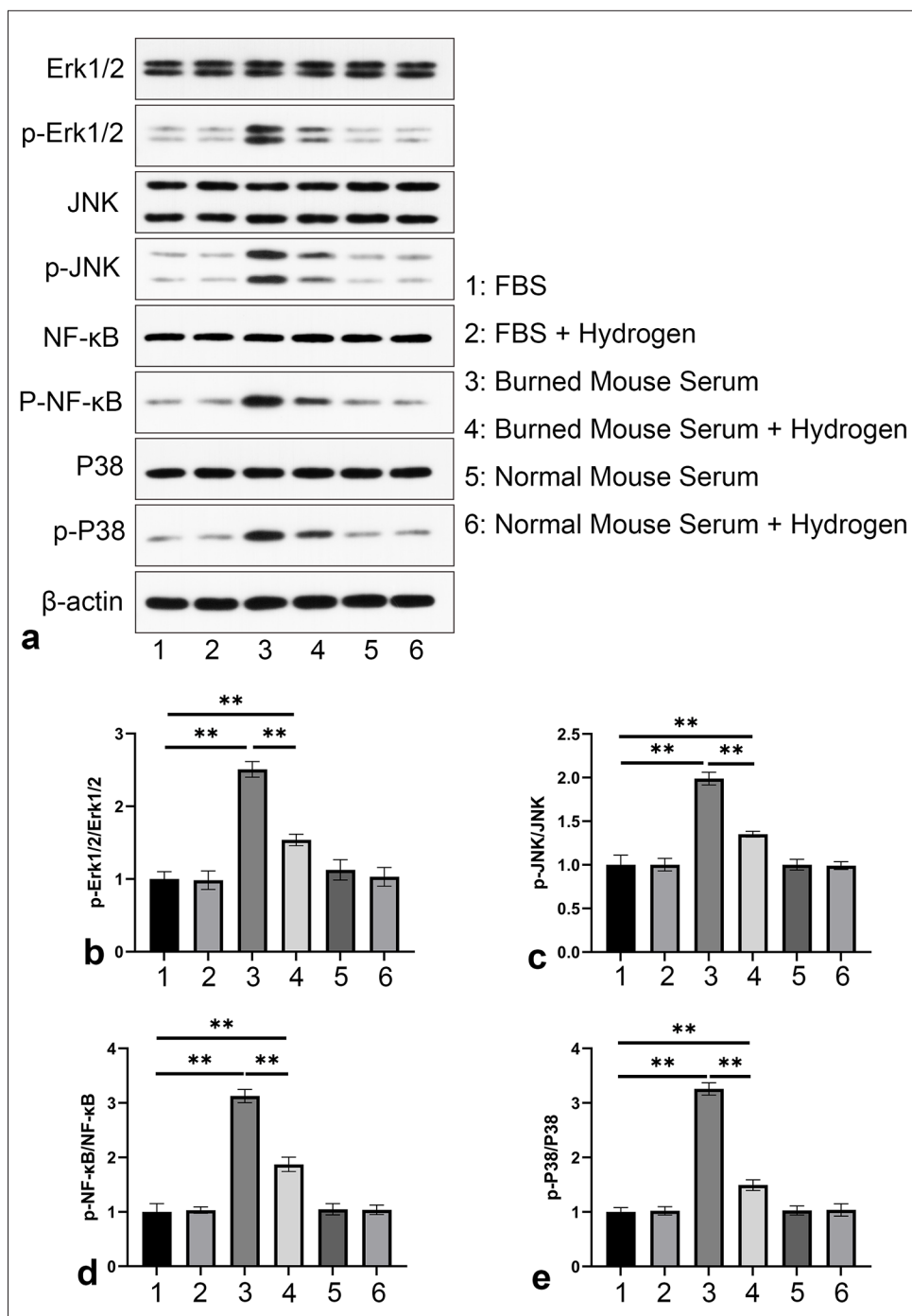The inflammatory and oxidative stress responses in the plasma and skin tissues of rats with burn sepsis were

Figure 3: Molecular mechanisms underlying the regulation of fibroblast responses through burn serum and hydrogen gas treatment. (a) WB and quantitative analysis of (b) p-Erk1/2, Erk1/2, (c) p-JNK, JNK, (d) p-NF-κB, NF-κB, and (e) p-P38, P38. **$P < 0.01$, compared with normal FBS group, $n = 3$. WB: Western blotting, H$_2$: Hydrogen gas, NF-κB: Nuclear factor-kappa B.

regulated through hydrogen gas treatment. Compared with that of the normal group, the plasma levels of pro-inflammatory cytokines TNF-α [Figure 5a], IL-1β [Figure 5b], and IL-6 [Figure 5c] were significantly elevated in the burn-sepsis control group ($P < 0.01$), which indicates a robust inflammatory response without hydrogen gas treatment. The levels of these cytokines were notably reduced in the burn sepsis + hydrogen gas group
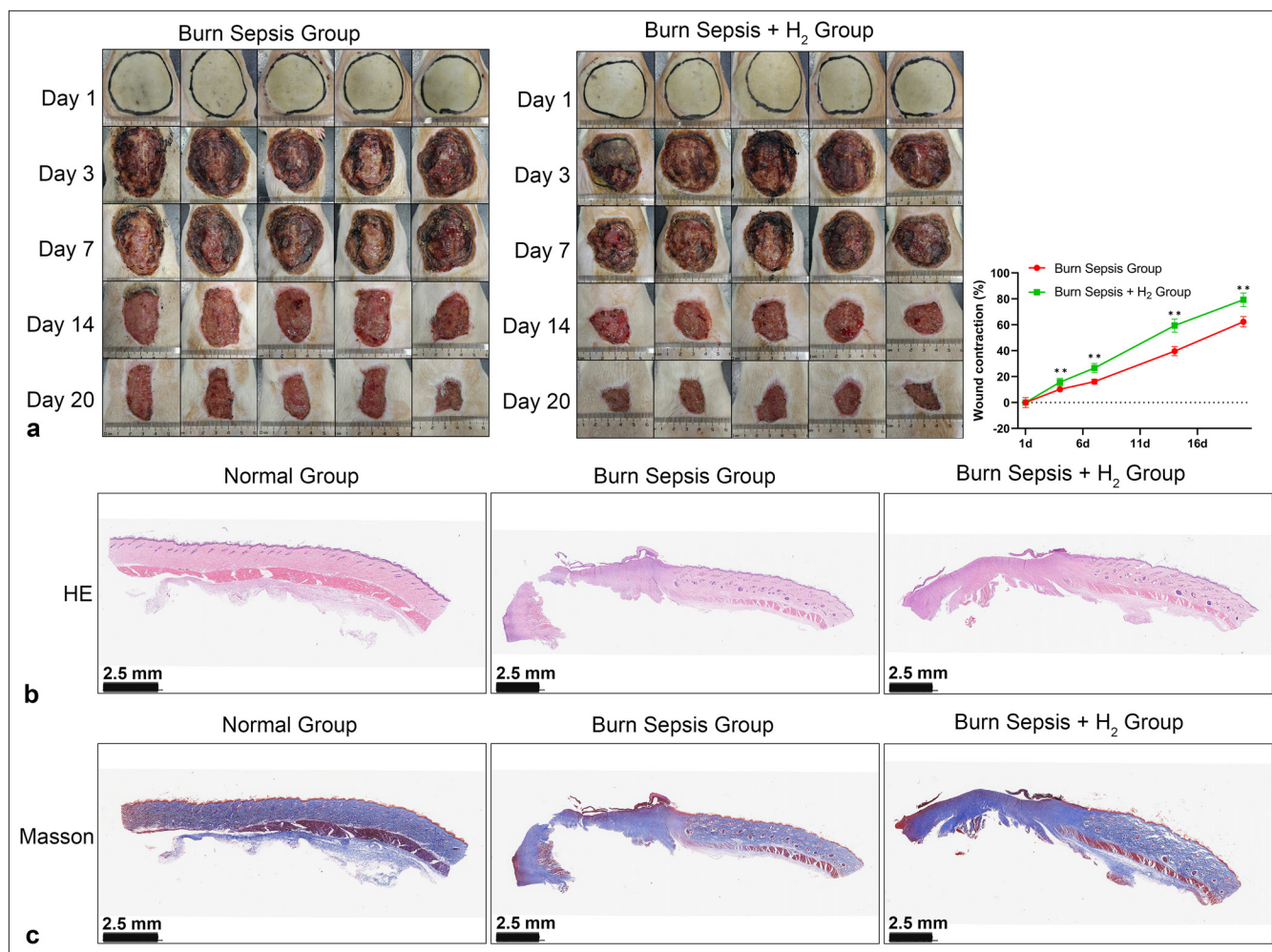
Figure 4: Effect of H₂ treatment on wound healing in burn sepsis: (a) Wound healing rates in rats with burn sepsis following H₂ treatment. (b) HE staining, 40× and (c) Masson's trichrome staining, 40× of burn wounds. *Comparison with burn sepsis group: **$P < 0.01$, $n = 5$. H₂: Hydrogen gas, HE: Hematoxylin and eosin. Scale bar: 2.5 mm.

($P < 0.05$), which suggests the anti-inflammatory effect of hydrogen gas. The level of the oxidative stress marker MDA [Figure 5d] was elevated in the burn-sepsis control group, which reflects an increase in lipid peroxidation alleviated by hydrogen gas treatment ($P < 0.01$). Conversely, the levels of the antioxidant enzyme SOD [Figure 5e] and the antioxidant molecule GSH [Figure 5f] were decreased in the burn-sepsis control group ($P < 0.01$). This condition indicates the depletion of endogenous antioxidant defense mechanisms, which were partially restored by hydrogen gas treatment. In addition, the plasma levels of the late inflammatory mediator HMGB1 were elevated in the burn-sepsis control group and reduced following hydrogen gas treatment ($P < 0.01$) [Figure 5g].

Similar to the plasma results, the skin tissue levels of TNF-α [Figure 5h], IL-1β [Figure 5i], and MDA [Figure 5j] were significantly elevated in the burn-sepsis control group and

reduced by hydrogen gas treatment ($P < 0.01$). The SOD activity [Figure 5k] and GSH levels [Figure 5l] of the skin tissue were decreased in the burn-sepsis control group ($P < 0.01$), which indicates impaired skin antioxidant capacity; such condition was improved by hydrogen gas treatment ($P < 0.01$). These results indicate that hydrogen gas possesses a potential therapeutic effect in mitigating systemic and local inflammatory and oxidative stress responses induced by burn sepsis compared with the normal group.

Hydrogen gas treatment modulated the activation of key signaling pathways involved in inflammatory and stress responses in burn sepsis

The activation of critical signaling pathways involved in inflammatory and stress responses in burn sepsis was regulated by hydrogen gas treatment. Figure 6a presents the
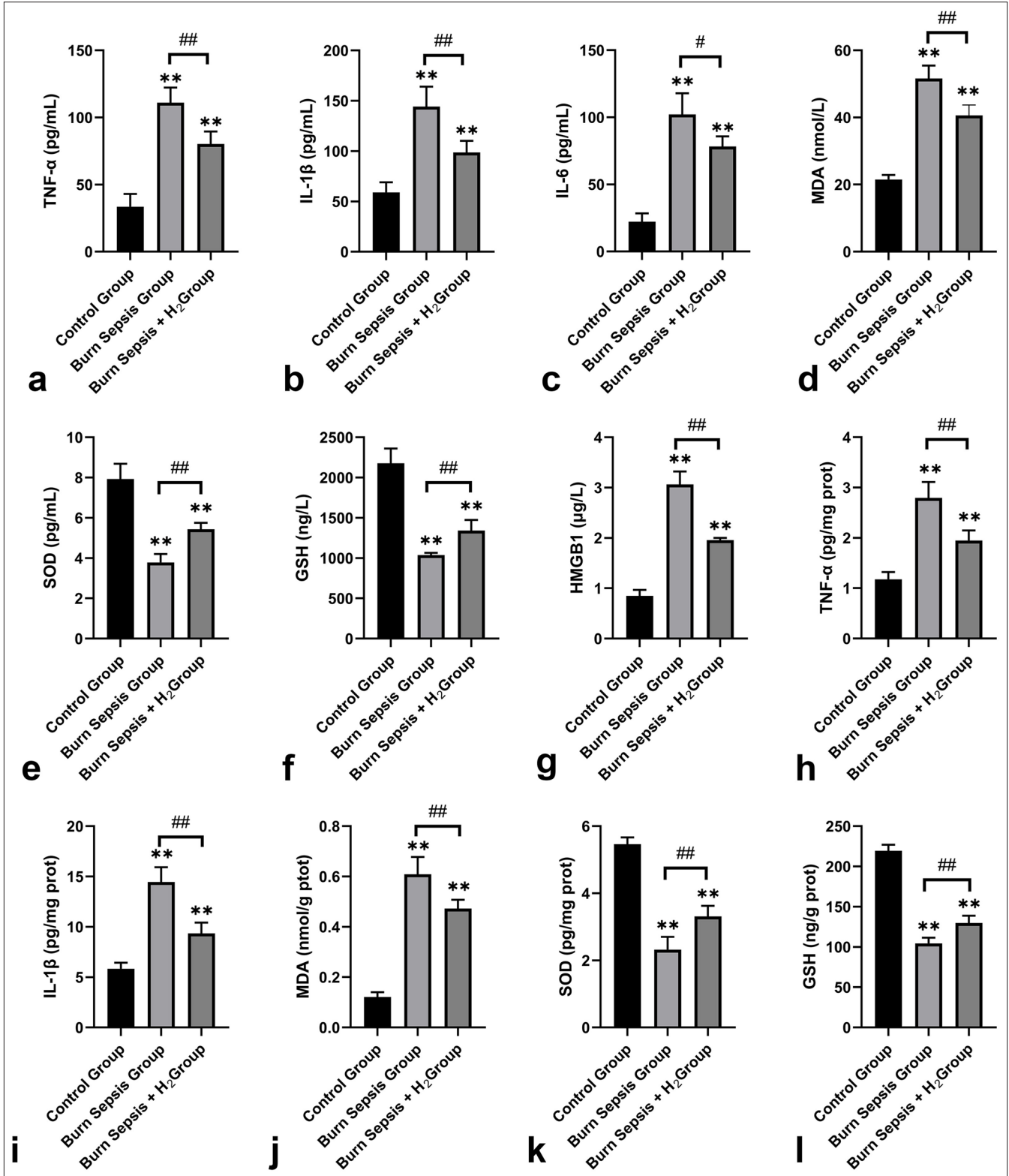
Figure 5: Inflammatory and Oxidative Stress Markers in Plasma and Skin Tissues Detected by ELISA. (a-g) Variations in the levels of TNF-α, IL-1β, IL-6, HMGB1, MDA, SOD, and GSH in plasma. (h-l) Variations in the levels of TNF-α, IL-1β, MDA, SOD, and GSH in skin tissues. *Comparison with normal group: **$P < 0.01$; #Comparison with burn-sepsis control group: #$P < 0.05$, ##$P < 0.01$, $n = 5$. ELISA: Enzyme-linked immunosorbent assay, MDA: Malondialdehyde, SOD: Superoxide dismutase, GSH: Glutathione, HMGB1: High-mobility group box 1 protein, FBS: Fetal bovine serum, IL-1β: Interleukin 1 beta, TNF-α: Tumor necrosis factor-alpha.
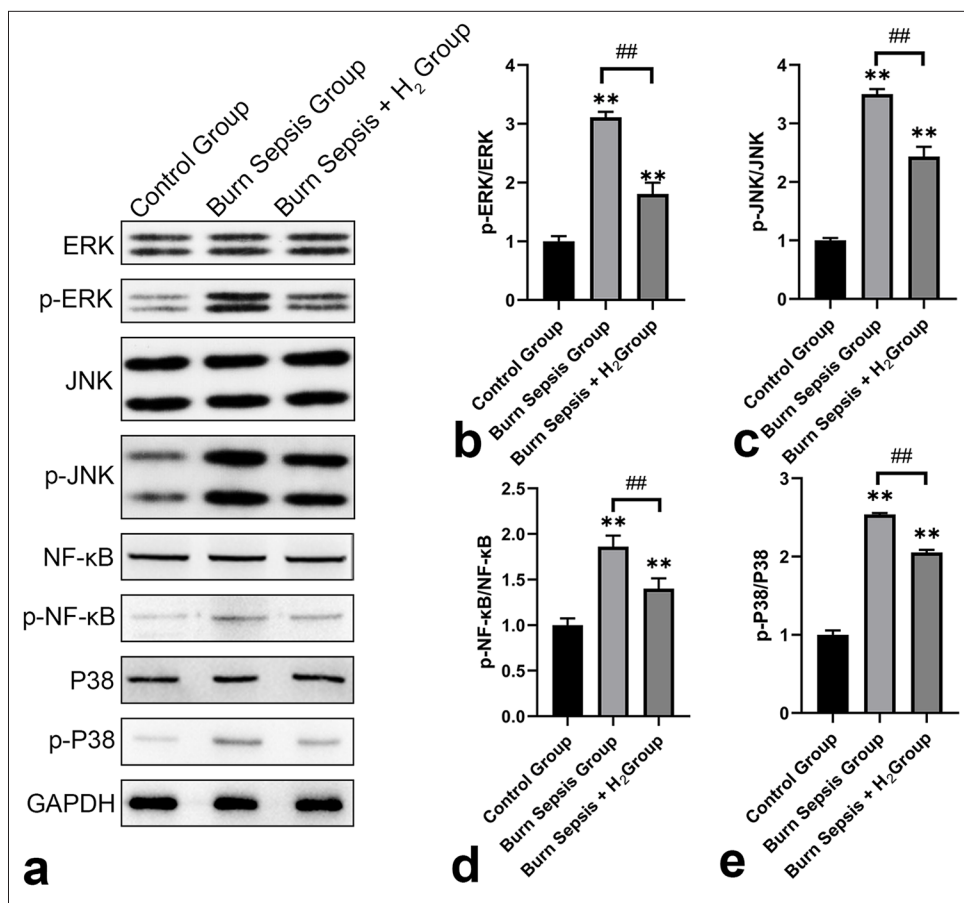
Figure 6: WB and quantitative analysis of key protein marker changes promoted by H$_2$ treatment in burn sepsis. (a) p-Erk1/2/Erk1/2, (b) p-JNK/JNK, (c) p-NF-κB/NF-κB, (d) p-P38/P38, and (e) representative WB bands of p-JNK, JNK, p-Erk1/2, Erk1/2, p-P38, P38, p-NF-κB, and NF-κB, with three replicates each. **Comparison with normal group: **$P < 0.01$; ##Comparison with burn-sepsis control group: ##$P < 0.01$, $n = 3$. WB: Western blotting, H$_2$: Hydrogen gas, NF-κB: Nuclear factor-kappa B.

original WB data on the aforementioned proteins. The ratio of P-Erk1/2/Erk1/2 in the burn sepsis control group was significantly higher than that in the normal group ($P < 0.01$), indicating an increase in Erk1/2 activity, which is associated with various cellular responses, including apoptosis and excessive inflammation. Hydrogen treatment significantly decreased this ratio ($P < 0.01$), which suggests an inhibitory effect on the Erk1/2 signaling pathway [Figure 6b]. Similarly, the ratio of p-JNK/JNK was markedly increased in the burn-sepsis control group ($P < 0.01$). This scenario reflects the activation of the JNK pathway, which is involved in stress responses and cell apoptosis. After hydrogen gas administration, this ratio was significantly reduced ($P < 0.01$), which indicates a protective effect against JNK-mediated cellular stress [Figure 6c]. In the burn-sepsis control group, the ratio of p-NF-κB/NF-κB was significantly upregulated ($P < 0.01$), which implies the activation of the NF-κB pathway, a central regulator of inflammation.

Hydrogen gas treatment significantly decreased this ratio ($P < 0.01$), which suggests that hydrogen gas may exert an anti-inflammatory effect by inhibiting the NF-κB signaling pathway [Figure 6d]. Likewise, in the burn-sepsis control group, the ratio of p-P38/P38 was significantly elevated ($P < 0.01$), which denotes the activation of the P38 pathway, which participates in inflammatory responses and cell death. Hydrogen gas treatment significantly reduced this ratio ($P < 0.01$), which suggests a mitigating effect on p38-mediated inflammatory responses [Figure 6e].

DISCUSSION

Burn wound sepsis represents an extremely serious clinical syndrome commonly triggered by infections at burn sites and leads to systemic inflammatory response and multiple organ dysfunctions. The incidence and mortality rates of sepsis in burn patients are notably high, which poses an important

challenge in burn treatment. Despite crucial advances in modern medicine regarding anti-infection, supportive therapies, and immunomodulation, the complications and mortality associated with sepsis remain elevated. Therefore, the exploration of new therapeutic strategies to improve the prognosis of burn wound sepsis has substantial clinical significance.[39]

Given the severity of sepsis and the limitations of current treatments, this study aimed to evaluate the potential of hydrogen gas as a novel treatment for burn wound sepsis. Hydrogen, as a selective antioxidant, has demonstrated anti-inflammatory, antioxidative, and healing-promoting properties in various disease models. However, its application in burn sepsis has not been thoroughly investigated. Thus, this work sought to elucidate the potential therapeutic mechanism of hydrogen by examining its effects on the inflammatory response, oxidative stress, and wound healing of a rat model of burn wound sepsis, and the findings provide scientific evidence for its clinical application. Our results indicate that hydrogen treatment significantly improved several adverse outcomes associated with burn wound sepsis, including delayed wound healing, exacerbated inflammatory responses, and increased oxidative stress. These outcomes suggest the potential of hydrogen as a promising adjunctive therapy in the management of post-burn sepsis.

Our study showed that hydrogen effectively alleviated the fibroblast proliferation inhibition and increased apoptosis induced by burn serum [Figure 1], consistent with the previously reported anti-apoptotic properties of hydrogen.[33,40] In addition, hydrogen-treated rats exhibited accelerated wound healing [Figure 4]. Enhanced wound contraction rates and improved histological results, including better tissue structure and collagen deposition, indicate the positive role of hydrogen in wound healing. These results are consistent with previous findings on hydrogen's promotion of wound healing.[12,41]

The mechanism by which hydrogen promotes wound healing may be closely related to its anti-inflammatory, antioxidative, and proliferative properties. Hydrogen's protective effects on fibroblasts are further supported by reductions in the levels of inflammatory cytokines and oxidative stress markers in plasma and skin tissue [Figures 2 and 5]. These results align with hydrogen's established anti-inflammatory and antioxidative properties.[42] The reductions in the levels of TNF-α, IL-1β, and IL-6 suggest that hydrogen may suppress the inflammatory cascade triggered by burn wound sepsis.[43] Furthermore, the decrease in the level of late-stage inflammatory mediator HMGB1 underscores the anti-inflammatory action of hydrogen.[44] Hydrogen's capability to mitigate oxidative stress induced by burn wound sepsis was demonstrated by the reduced MDA levels and increased SOD and GSH levels in cellular and animal models. These findings are consistent with hydrogen's capacity to combat oxidative stress by reducing lipid peroxidation and enhancing antioxidant enzyme activity. The reduction in the amount of inflammatory cytokines and the improvement in oxidative stress markers suggest that hydrogen may help restore the immune balance disrupted by burn wound sepsis.[45] This condition is crucial to prevent the progression of sepsis to septic shock and MODS, which are the primary causes of death in burn wound sepsis patients.

Hydrogen's regulation of key signaling pathways was further explored [Figures 3 and 6]. The downregulation of p-JNK, p-P38, p-NF-κB, and p-ERK in fibroblasts after hydrogen treatment, suggests that hydrogen may exert its therapeutic effects through the modulation of these signaling pathways. The activation of JNK, P38, and NF-κB is closely related to inflammation and cellular stress, whereas that of ERK is associated with apoptosis and proliferation.[46,47] Hydrogen's capability to modulate these pathways may constitute a core mechanism for its therapeutic effects on burn wound sepsis.

The mechanisms by which hydrogen exerts its effects are complex and may involve multiple pathways and cellular targets. Further investigation, including molecular and cellular studies, is required to elucidate the exact mechanisms. In addition, although our study demonstrated the therapeutic potential of hydrogen in a rat model of burn wound sepsis, the translation of findings to clinical practice remains to be validated. Future research should focus on determining the optimal dosage, administration route, and treatment timing of hydrogen therapy for patients with burn wound sepsis.

SUMMARY

This study provides strong evidence for the therapeutic effects of hydrogen on burn-induced sepsis. By modulating inflammation, oxidative stress, and wound healing, hydrogen therapy can potentially improve clinical outcomes in this critical condition. Future research should further elucidate its mechanisms of action and translate these findings into clinical practice.

AVAILABILITY OF DATA AND MATERIALS

The datasets used or analyzed during the present study are available from the corresponding author on reasonable request.

ABBREVIATIONS

CST: Cell signaling technology
GSH: Glutathione
H₂: Hydrogen gas
HE: Hematoxylin and eosin

IACUC: Institutional Animal Care and Use Committee
MDA: Malondialdehyde
MODS: Multiple organ dysfunction syndrome
RSF cells: Rat skin fibroblasts
SD: Sprague-Dawley
SIRS: Systemic inflammatory response syndrome
SOD: Superoxide dismutase
TBSA: Total body surface area

AUTHOR CONTRIBUTIONS

PY: Study conception and design; NH and GWW: Data collection; PY: Experimental studies; GWW, SQC and ZPZ: Analysis and interpretation of results; PY and NH: Draft manuscript preparation. All authors reviewed the results and approved the final version of the manuscript. All authors meet the ICMJE authorship criteria.

ETHICS APPROVAL AND CONSENT TO PARTICIPATE

The experimental protocols involving animal subjects strictly adhered to the guidelines established by the Institutional Animal Care and Use Committee and were ethically vetted and approved by the Ethics Committee of Jinling Hospital, Affiliated Hospital of Medical School, Nanjing University, China. (Approval Number: DBZQZYY23BBJ0081). All measures were diligently implemented to mitigate and minimize any potential distress or suffering experienced by the animals throughout the study. Since this study does not involve human subjects, informed consent to participate is not required.

ACKNOWLEDGMENT

FUNDING

CONFLICT OF INTEREST

The authors declare no conflict of interest.

EDITORIAL/PEER REVIEW

To ensure the integrity and highest quality of CytoJournal publications, the review process of this manuscript was conducted under a **double-blind model** (authors are blinded for reviewers and vice versa) through an automatic online system.

REFERENCES

1. Zhai G, Wang Y, Han P, Xiao T, You J, Guo C, *et al.* Drug loaded marine polysaccharides-based hydrogel dressings for treating skin burns. Int J Biol Macromol 2024;281:135779.
2. Qianqian O, Songzhi K, Yongmei H, Xianghong J, Sidong L, Puwang L, *et al.* Preparation of nano-hydroxyapatite/chitosan/tilapia skin peptides hydrogels and its burn wound treatment. Int J Biol Macromol 2021;181:369-77.
3. Liu J, Liu Y, Liu S, Zhang Q, Zheng J, Niu Y, *et al.* Hypocoagulation induced by broad-spectrum antibiotics in extensive burn patients. Burns Trauma 2019;7:13.
4. Bhavani SV, Spicer A, Sinha P, Malik A, Lopez-Espina C, Schmalz L, *et al.* Distinct immune profiles and clinical outcomes in sepsis subphenotypes based on temperature trajectories. Intensive Care Med 2024;50:2094-104.
5. Blet A, Deniau B, Santos K, van Lier D, Azibani F, Wittebole X, *et al.* Monitoring circulating dipeptidyl peptidase 3 (DPP3) predicts improvement of organ failure and survival in sepsis: A prospective observational multinational study. Crit Care 2021;25:61.
6. Yang T, Fang H, Lin D, Yang S, Luo H, Wang L, *et al.* Ganoderma Lucidum polysaccharide peptide (GL-PP2): A potential therapeutic agent against sepsis-induced organ injury by modulating Nrf2/NF-kappaB pathways. Int J Biol Macromol 2024;285:138378.
7. Guo K, Zhou TT, Luo SH, Liu YC, Liu Y, Li SH. Leucosceptrane sesterterpenoids as a new type of natural immunosuppressive agents in treating sepsis. J Med Chem 2024;67:513-28.
8. Liu H, Pan D, Li P, Wang D, Xia B, Zhang R, *et al.* Loss of ZBED6 protects against sepsis-induced muscle atrophy by upregulating DOCK3-mediated RAC1/PI3K/AKT signaling pathway in pigs. Adv Sci (Weinh) 2023;10:e2302298.
9. Hu S, Huang M, Mao S, Yang M, Ju H, Liu Z, *et al.* Serinc2 deficiency exacerbates sepsis-induced cardiomyopathy by enhancing necroptosis and apoptosis. Biochem Pharmacol 2023;218:115903.
10. Ding J, Xu K, Xu H, Ji J, Qian Y, Shen J. Advances in gas therapeutics for wound healing: Mechanisms, delivery materials, and prospects. Small Struct 2024;5:2300151.
11. Brakenridge SC, Chen UI, Loftus T, Ungaro R, Dirain M, Kerr A, *et al.* Evaluation of a multivalent transcriptomic metric for diagnosing surgical sepsis and estimating mortality among critically ill patients. JAMA Netw Open 2022;5:e2221520.
12. Wu L, Yang X, Jia H, Xiao L, Gao C, Hu Z, *et al.* Freestanding hydrogen-bonded organic framework membrane for efficient wound healing. Adv Mater 2024;36:e2411229.
13. Chi H, Wu W, Bao H, Wu Y, Hu N. Self-driven Janus Ga/Mg micromotors for reducing deep bacterial infection in the treatment of periodontitis. Adv Healthc Mater 2024;e2404303.
14. Wu Q, Ghosal K, Kana'An N, Roy S, Rashed N, Majumder R, *et al.* On-demand imidazolidinyl urea-based tissue-like, self-healable, and antibacterial hydrogels for infectious wound care. Bioact Mater 2024;44:116-30.
15. Liao Y, Zhang Z, Zhao Y, Zhang S, Zha K, Ouyang L, *et al.* Glucose oxidase: An emerging multidimensional treatment option for diabetic wound healing. Bioact Mater 2024;44:131-51.
16. Zhao P, Dang Z, Liu M, Guo D, Luo R, Zhang M, *et al.* Molecular hydrogen promotes wound healing by inducing early epidermal stem cell proliferation and extracellular matrix deposition. Inflamm Regen 2023;43:22.
17. Chen H, Guo Y, Zhang Z, Mao W, Shen C, Xiong W, *et al.*

Symbiotic algae-bacteria dressing for producing hydrogen to accelerate diabetic wound healing. Nano Lett 2022;22:229-37.

18. Atiakshin D, Soboleva M, Nikityuk D, Alexeeva N, Klochkova S, Kostin A, *et al.* Mast cells in regeneration of the skin in burn wound with special emphasis on molecular hydrogen effect. Pharmaceuticals (Basel) 2023;16:348.

19. Chen HG, Xie KL, Han HZ, Wang WN, Liu DQ, Wang GL, *et al.* Heme oxygenase-1 mediates the anti-inflammatory effect of molecular hydrogen in LPS-stimulated RAW 264.7 macrophages. Int J Surg 2013;11:1060-6.

20. Sun R, Zhao N, Wang Y, Su Y, Zhang J, Wang Y, *et al.* High concentration of hydrogen gas alleviates Lipopolysaccharide-induced lung injury via activating Nrf2 signaling pathway in mice. Int Immunopharmacol 2021;101:108198.

21. Yu Y, Yang Y, Yang M, Wang C, Xie K, Yu Y. Hydrogen gas reduces HMGB1 release in lung tissues of septic mice in an Nrf2/HO-1-dependent pathway. Int Immunopharmacol 2019;69:11-8.

22. Xu M, Wu G, You Q, Chen X: The Landscape of smart biomaterial-based hydrogen therapy. Adv Sci (Weinh) 2024;11:e2401310.

23. Liu J, Li G, Chen YZ, Zhang LD, Wang T, Wen ZL, *et al.* Effects of rhubarb on the expression of glucocorticoids receptor and regulation of cellular immunity in burn-induced septic rats. Chin Med J (Engl) 2019;132:1188-93.

24. Li C, Xiong Y, Fu Z, Ji Y, Yan J, Kong Y, *et al.* The direct binding of bioactive peptide Andersonin-W1 to TLR4 expedites the healing of diabetic skin wounds. Cell Mol Biol Lett 2024;29:24.

25. Wang L, Yu X, Li H, He D, Zeng S, Xiang Z. Cell and rat serum, urine and tissue metabolomics analysis elucidates the key pathway changes associated with chronic nephropathy and reveals the mechanism of action of rhein. Chin Med 2023;18:158.

26. Lo T, Lee Y, Tseng CY, Hu Y, Connelly MA, Mantzoros CS, *et al.* Daily transient coating of the intestine leads to weight loss and improved glucose tolerance. Metabolism 2022;126:154917.

27. Ahmadpour F, Rasouli HR, Talebi S, Golchin D, Esmailinejad MR, Razie A. Effects of exosomes derived from fibroblast cells on skin wound healing in Wistar rats. Burns 2023;49:1372-81.

28. Liu X, Wang S, Liu G, Wang Y, Shang S, Zou G, *et al.* Advancing the clinical assessment of glomerular podocyte pathology in kidney biopsies via super-resolution microscopy and angiopoietin-like 4 staining. Theranostics 2025;15:784-803.

29. Chen F, Lang L, Yang J, Yang F, Tang S, Fu Z, *et al.* SMAC-armed oncolytic virotherapy enhances the anticancer activity of PD1 blockade by modulating PANoptosis. Biomark Res 2025;13:8.

30. Zhou C, Yang MJ, Shi P, Li ZQ, Li YR, Guo YJ, *et al.* Ascorbic acid transporter MmSLC23A2 functions to inhibit apoptosis via ROS scavenging in hard clam (*Mercenaria mercenaria*) under acute hypo-salinity stress. Int J Biol Macromol 2025;302:139483.

31. Jianguo F, Menghong L, Xin Z, Pijun Y, Yunxiao L, Maohua W, *et al.* RBM3 Accelerates wound healing of skin in diabetes through ERK1/2 signaling. Curr Mol Pharmacol 2024;17:e18761429260980.

32. Li J, Ruan S, Jia J, Li Q, Jia R, Wan L, *et al.* Hydrogen attenuates postoperative pain through Trx1/ASK1/MMP9 signaling pathway. J Neuroinflammation 2023;20:22.

33. Zou R, Nie C, Pan S, Wang B, Hong X, Xi S, *et al.* Co-administration of hydrogen and metformin exerts cardioprotective effects by inhibiting pyroptosis and fibrosis in diabetic cardiomyopathy. Free Radic Biol Med 2022;183:35-50.

34. Zhang Y, Zhang J, Zhu YU, Cai B. Platelet rich plasma-complexed hydrogel glue enhances skin wound healing in a diabetic rat model. Biocell 2022;46:1329-38.

35. Kim Y, Jung KY, Kim YH, Xu P, Kang BE, Jo Y, *et al.* Inhibition of SIRT7 overcomes sorafenib acquired resistance by suppressing ERK1/2 phosphorylation via the DDX3X-mediated NLRP3 inflammasome in hepatocellular carcinoma. Drug Resist Updat 2024;73:101054.

36. Liu N, Zhang X, Li N, Zhou M, Zhang T, Li S, *et al.* Tetrahedral framework nucleic acids promote corneal epithelial wound healing *in vitro* and *in vivo*. Small 2019;15:e1901907.

37. Zhang R, Xu B, Zhang N, Niu J, Zhang M, Zhang Q, *et al.* Spinal microglia-derived TNF promotes the astrocytic JNK/CXCL1 pathway activation in a mouse model of burn pain. Brain Behav Immun 2022;102:23-39.

38. Zhou R, Ying J, Qiu X, Yu L, Yue Y, Liu Q, *et al.* A new cell death program regulated by toll-like receptor 9 through p38 mitogen-activated protein kinase signaling pathway in a neonatal rat model with sepsis associated encephalopathy. Chin Med J (Engl) 2022;135:1474-85.

39. Pineda-Reyes R, Neil BH, Orndorff J, Williams-Bouyer N, Netherland MJ, Hasan NA, *et al.* Clinical presentation, antimicrobial resistance, and treatment outcomes of Aeromonas human infections: A 14-year retrospective study and comparative genomics of two isolates from fatal cases. Clin Infect Dis 2024;79:1144-52.

40. Li L, Xu Z, Ni H, Meng Y, Xu Y, Xu H, *et al.* Hydrogen-rich water alleviates asthma airway inflammation by modulating tryptophan metabolism and activating aryl hydrocarbon receptor via gut microbiota regulation. Free Radic Biol Med 2024;224:50-61.

41. Zhao P, Cai Z, Zhang X, Liu M, Xie F, Liu Z, *et al.* Hydrogen attenuates inflammation by inducing early M2 macrophage polarization in skin wound healing. Pharmaceuticals (Basel) 2023;16:885.

42. Stachowicz A, Wisniewska A, Czepiel K, Pomierny B, Skorkowska A, Kusnierz-Cabala B, *et al.* Mitochondria-targeted hydrogen sulfide donor reduces atherogenesis by changing macrophage phenotypes and increasing UCP1 expression in vascular smooth muscle cells. Biomed Pharmacother 2024;180:117527.

43. Ohsawa I, Ishikawa M, Takahashi K, Watanabe M, Nishimaki K, Yamagata K, *et al.* Hydrogen acts as a therapeutic antioxidant by selectively reducing cytotoxic oxygen radicals. Nat Med 2007;13:688-94.

44. Yang M, Dong Y, He Q, Zhu P, Zhuang Q, Shen J, *et al.* Hydrogen: A novel option in human disease treatment. Oxid Med Cell Longev 2020;2020:8384742.

45. Lee D, Choi JI. Hydrogen-rich water improves cognitive ability and induces antioxidative, antiapoptotic, and anti-inflammatory effects in an acute ischemia-reperfusion injury

mouse model. Biomed Res Int 2021;2021:9956938.

46. Lavoie H, Gagnon J, Therrien M. ERK signalling: A master regulator of cell behaviour, life and fate. Nat Rev Mol Cell Biol 2020;21:607-32.

47. Mebratu Y, Tesfaigzi Y. How ERK1/2 activation controls cell proliferation and cell death: Is subcellular localization the answer? Cell Cycle 2009;8:1168-75.